Chapter 7: Post-flight Analysis of the Argon Filled Ion Chamber

H. Tai*, P. Goldhagen, I. W. Jones*, J. W. Wilson*, D. L. Maiden*, J. L. Shinn***

***NASA Langley Research Center, Hampton, Virginia 23681-0001**

****DOE Environmental Measurements Laboratory, New York, NY 20014**

Atmospheric Ionizing Radiation (AIR) ER-2 Stratospheric Measurements Post-flight Analysis: The Argon Filled Ion Chamber

Preface

Atmospheric ionizing radiation is a complex mixture of primary galactic and solar cosmic rays and a multitude of secondary particles produced in collision with air nuclei. The first series of Atmospheric Ionizing Radiation (AIR) measurement flights on the NASA research aircraft ER-2 took place in June 1997. The ER-2 flight package consisted of fifteen instruments from six countries and were chosen to provide varying sensitivity to specific components. These AIR ER-2 flight measurements are to characterize the AIR environment during solar minimum to allow the continued development of environmental models of this complex mixture of ionizing radiation. This will enable scientists to study the ionizing radiation health hazard associated with the high-altitude operation of a commercial supersonic transport and to allow estimates of single event upsets for advanced avionics systems design. The argon filled ion chamber representing about 40 percent of the contributions to radiation risks are analyzed herein and model discrepancies for solar minimum environment are on the order of 5 percent and less. Other biologically significant components remain to be analyzed.

Introduction

The AIR ER-2 flight measurements are part of a program established by the High-Speed Research (HSR) program to study the radiation risk associated with the high-altitude flight operation of a commercial supersonic transport (Foelsche et al. 1974, FAA 1975, Schaefer 1968). This program also includes the development of an AIR predictive code, and a national assessment of the radiation health hazard associated with high altitude flight. The High Speed Research Project Office (HSRPO) at the Langley Research Center has been delegated the responsibility by NASA Headquarters, Washington DC, to develop key technologies to enable the development of an economically viable and environmentally acceptable High Speed Civil Transport (HSCT, a supersonic airliner) by the year 2005. The leading candidates for the new HSCT supersonic transport is a Mach 2.4 configuration which will cruise efficiently at altitudes between 18 to 20 kilometers. Marketing networks show about 60% of HSCT operations will occur at northern geomagnetic latitudes. Because of the high-altitude at cruise and predominately northern-latitude operating networks, the aircraft is less protected from the natural environment of galactic and solar cosmic rays. Thus arises the need to access the possible high-altitude radiation health hazard to which the HSCT crew and passengers will be subjected (O'Brien and Friedberg 1994). The National Council on Radiation Protection and Measurements (NCRP) recommended that a program be established to reduce the uncertainties in risk estimates for high altitude flight to levels comparable with those of ground based occupational exposure risks (1993, 1995).

Hazardous radiation comes in two forms: non-ionizing, (ultraviolet, infrared and microwave) and ionizing, (gamma, x-rays, and subatomic particles). Both types are dangerous because of their adverse biological effects when they pass through body tissue. At flight altitudes, cosmic radiation consists of high-energy subatomic particles, originating for the most part outside the solar system, which collide with and disrupt atoms of nitrogen, oxygen, and other constituents of the atmosphere. Additional subatomic particles are produced from these collisions. The particles from beyond the solar system and their secondary particles produced in the atmosphere are referred to collectively as galactic cosmic radiation. Another source of in-flight ionizing radiation is solar cosmic radiation, which arises primarily from solar particle events (resulting from coronal mass ejection). Although charged particles are continuously being ejected from the sun, they are usually too low in energy to contribute to the radiation level at flight altitudes. However, on infrequent and unpredictable occasions, the numbers and energies of ejected solar particles are high enough to increase substantially the dose rate at these altitudes. The understanding of such complex radiation environment at high altitudes requires a diverse array of instruments that are not available at any one laboratory. A national and international collaboration has been devised to ensure that the environmental components are adequately covered within a reasonable budget with existing instrumentation and within the payload requirements of the NASA ER-2 aircraft. The (AIR) ER-2 flight measurements took place from June 2 to June 15, 1997. There were a total of five science mission flights (ER-2 Sortie 97-105 to 97-109) and one engineering flight (flight 97-104) flown. A total of 37.2 hours of airtime were logged. Instruments on board were selected based the recommendations by the National Council on Radiation and Protection (NCRP) (1995) to help provide a basis for radiation monitoring during high altitude operations of the ER-2 aircraft. This whole airborne campaign is coordinated by the National Aeronautics and Space Administration Langley Research Center (NASA/LaRC) in collaboration with the US Department of Energy (DOE), Environmental Measurements Laboratory (EML); the NASA Johnson Space Center; the German Aerospace Research Establishment (DLR); Canadian Royal Military College (RMC); Canadian Defense Research Establishment Ottawa (DREO); UK National Radiological Protection Board (NRPB); the Boeing Company; the University of Pisa, Italy; the University of San Francisco, California; the National Institute of Occupation and Health (NIOSH); and the Federal Aviation Agency (FAA), Civil Aeromedical Institute. The flight package placement on the ER-2 aircraft is shown in figure 1.

AIR Model Version 0

The AIR model version 0 is the parametric fit to data gathered by the Langley Research Center studies of the radiation at SST altitudes in the years 1965 to 1971 covering the rise and decline of solar cycle 20. Scaling of the data with respect to geomagnetic cutoff, altitude, and modulation of the Deep River Neutron Monitor was found to allow mapping of the environment to all locations at all times resulting in an empirically based model named AIR model Version 0 (Wilson et al. 1991). The basic data consisted of tissue equivalent ion chamber rates, fast neutron spectrometer, and nuclear emulsion detection of nuclear reaction products in amino acids (gel). The model was based on global surveys with airplane and balloons.

The latitude surveys by balloons and aircraft are shown for the transition maximum in figure 2. The curves in the figure are our approximation to the data and given by

$$\phi(x,R,C) = f(R,C) \exp(-x/\lambda) - F(R,C) \exp(-x/\Lambda) \quad (1)$$

where

$$f(R,C) = \exp(250/\lambda)\ \phi_s\ (R,C) \quad (2)$$

$$F(R,C) = (\Lambda/\ \lambda)\ f(R,C) \exp(x_m/\ \Lambda - x_m/\ \lambda) \quad (3)$$

and

$$\Lambda = \lambda\ [\ 1 - \phi_m(R,C) \exp(x_m/\lambda)/f(R,C)] \quad (4)$$

where the transition maximum altitude x_m corresponds to

$$x_m = 50 + \ln\{2000 + \exp[-2(C-100)]\} \quad (5)$$

$$\phi_s\ (R,C) = 0.17 + [0.787 + 0.035\ (C - 100)] \exp(-R^2/25)$$
$$+ \{-0.107 - 0.0265\ (C-100)$$
$$+ 0.612 \exp[(C - 100)/3.73]\}\exp(-R^2/139.2) \quad (6)$$

$$\phi_m(R,C) = 0.23 + [1.1 + 0.167\ (C-100)] \exp(-R^2/81)$$
$$+ \{0.991 + 0.0501\ (C - 100)$$
$$+ 0.4 \exp[(C - 100)/3.73]\}\ \exp(-R^2/12.96) \quad (7)$$

In the above equations, R is the local cutoff rigidity (in units of GV) and C is the high-latitude neutron monitor count rate in percent of maximum. At depths below 250 g/cm^2, the neutrons attenuate with attenuation length (g/cm^2) given by

$$\lambda = 160+ 2\ R \quad (8)$$

The neutron environment model is shown in figure 2 in comparison to experimental measurements. The flux from 1-10 MeV is converted to dose equivalent and dose rates using 3.14 μSv-(cm^2/s)/hr and 0.5 μGy-(cm^2/s)/hr respectively. They are based on older dosimetric relations as described in Foelsche et al. (1974) using the ICRP 26 quality factor. The use of the ICRP 60 quality factor would increase the neutron dose equivalent by about 55 percent.

Unfortunately not all ion chamber data or all nuclear emulsion data were reduced. For our purpose we use the argon-filled ion chamber data to represent the altitude, latitude and solar cycle dependence of dose from all components except neutrons and use the available tissue equivalent ion chamber data as a guide. The ion chamber data of Neher and Anderson compiled by Curtis et al at the 1965 solar minimum (C = 98.3) in table 1 and the 1958 solar maximum (C = 80) in table 2. We have augmented the table with data from the work of Neher and Anderson. We note that the low-energy GCR had not fully recovered in the summer of 1965 with the result that the high-latitude ionization at high altitude is about 10 percent lower than that in 1954. Furthermore, the 1958 measurements near solar maximum covered only mid to high latitudes, and the low-latitude data in table 2 are likely to be about 10 percent too high at high altitudes. The ionization rates in tables 1 and 2 are the rates in air per atmosphere of pressure (directly related to the exposure unit Roentgen). The atmospheric ionization rates are interpolated in altitude, geomagnetic cutoff, and solar modulation and directly converted to exposure units and absorbed dose in tissue. The comparison with the tissue equivalent ion chamber requires the addition of the neutron absorbed dose rates and good consistency between this method and the tissue equivalent ion chamber has been demonstrated. Dose equivalent estimates require an estimate of the high LET components associated with charged particles and are found from the measurements in nuclear emulsion as shown in elsewhere. The corresponding average quality factor for the argon ion chamber dose is found to be

$$Q = 1+ 0.35 \exp(-x/416) - 0.194 \exp (-x/65) \quad (9)$$

This quality factor is to be applied only to the dose component derived from the argon ion chamber only. The approximate average quality factor (9) was fit to data at high latitudes and high altitudes and is a source of uncertainty elsewhere in the atmosphere.

Flight Trajectory and AIR Model Predictions

All ER-2 flights originated from Moffett Field, CA. In Fig. 3, a map of the ground track of the scheduled flights (flights code ER2 Sortie 97-105 to 97-109) are shown superimposed with radiation contours predicted by the AIR model.

Aside from the scientific data recorded by the instruments aboard the ER-2 plane that may take some time to get analyzed, the portion of navigation data, however are readily available. This important navigational information was recorded by on-board ER-2 instruments every second during the whole length of flight. This information consists of position (latitude and longitude), altitude (actually the atmospheric depth), pressure, heading, yaw and rolling angle, and ambient temperature. For analysis we need only selected data at every minute. What we have done is either choose the middle value or take the averaged value over the whole minute. They are not expected to differ significantly. In the following tables and graphs, average values are used. The science flight trajectory data and the corresponding AIR model values are given in an appendix.

Flight 97-104: This was approximately a two-hour, engineering flight required by the ER-2 operations office with pilot's choice of flight path (typically a race track around the home base). The aim is to check aircraft operational characteristics, and all aircraft and experimental instrumentation to assure everything is operating satisfactorily prior to the acquisition of science measurements.

Flight 97-105: This was approximately a six & one-half hour flight starting on June 5 at 15:50 on prescribed northern and easterly headings and return to home base over the reverse flight path. The aim for this flight was to determine if radiation measurements are being affected by the shielding characteristics of on-board aviation fuel, determine consistency of instrument readings, and take science data as a function of altitude along a constant-radiation, geomagnetic latitude line. The flight began at (37°24' N, 122°6' W) with a climb out of Moffett Field to the location (39°19'49" N, 121°27' W) where a easterly turn was executed (fig. 4 to 6) and continue to climb to cruise altitude near Wine Glass where the altitude was held constant at 20 km for about 20 minutes (fig. 6). Minor midcourse corrections were made to maintain a constant geomagnetic cutoff trajectory as shown in figure 7. A U-turn was made at (34 ° 39' N, 100 ° W) followed by a slow descent (500 ft/min) near Amarillo to 52,000 ft. which was maintained for 10 minutes. The pilot then climbed to normal cruise altitude along the prescribed flight path repeating the ground track on the return to Wine Glass making necessary course corrections to maintain constant geomagnetic cutoff. There was a thunder storm over north central New Mexico which had to be avoided on the return trip as seen in figure 3. Before reaching Wine Glass the pilot descended to the 20 km altitude as on the outbound trip and maintained that altitude for about 30 minutes. This was followed by return to cruise altitude and ending the flight by decent to Moffett Field. The model geomagnetic cutoff, dose equivalent, dose, 1-10 MeV neutron fluence rates are shown in figures 7 to 11.

Since the flight 97-105 was designed to fly parallel to geomagnetic latitude for the major leg (easterly heading and reverse), Fig. 7 shows the magnetic cut-off value was a horizontal straight line about 3.92-3.95 GV. Fig. 8 and 9 show the predictions for dose equivalent rate and dose rate from AIR model. Keep in mind that those rate values are a complicated function of flight coordinates as well as the altitude and other factors. Based on the figures, clearly the altitude factor alone suggests that the rate can change 12~15% from 16 km to 20 km in altitude. The AIR model predicts the neutron flux whose energy range is 1-10 MeV in Fig. 10 and air ionization rate in Fig. 11 along the flight path for this flight. That is, the AIR model predicts an altitude variation in the 1-10 MeV neutron flux of about 12 percent and in the air ionization rate of 11 percent at the approximate 3.935 GV cutoff.

Flight 97-106: This was approximately an eight hour flight on June 8 beginning at 15:52 on prescribed northern, western and southern headings. The aim was to obtain radiation measurements as a function of geomagnetic latitude to as far north as possible with an altitude excursion along a constant-radiation, geomagnetic latitude line at the extreme northern latitude location. The flight (fig. 3) began at (37 ° 24' N, 122 ° 6' W) with a climb out of Moffett Field and ascent to cruise altitude (fig. 12 to 14). Cruise to point near Ft. Nelson (59 ° 00' N, 116 ° 00' W) and turned west along constant geomagnetic cutoff trajectory (fig.

15) held altitude fixed (fig. 14) for 5 minutes after the west turn then executed a medium-rate descent (750 ft/min) to 52,000 ft. and maintained that altitude for 5 minutes (fig. 14). At location (60 ^{o} 00' N, 123 ^{o} 40' W) the aircraft turned south (toward Moffett Field) and ascended to cruise altitude until the decent at Moffett Field. The model geomagnetic cutoff, dose equivalent, dose, 1-10 MeV neutron fluence rates are shown in figures 15 to 19.

The purpose for this flight was to obtain radiation measurements as a function of geomagnetic latitude to as far north as possible with an altitude excursion along a constant-radiation, geomagnetic latitude line at the extreme northern latitude location. Fig. 13 shows that at the extreme northern latitude, magnetic cut-off values of 0.42-0.44 GV were achieved where the altitude survey was performed. Comparing Fig. 14-16 with Fig. 6-9, for the flight 97-106 route, the AIR model predicts much higher radiation values than for the flight 97-105 route. In other words, Flight 97-106, in a sense from the radiation safety point of view, flies a less safe route than flight 97-105 which was expected. The altitude survey at approximately 0.43 GV shows a variation on the order of 11 percent in 1-10 MeV neutron flux and 23 percent for the air ionization rate. Since the primary purpose of flight 97-106 was to perform a latitude survey, we see that the high altitude variation in the environment during the cruise portion of the flight along the northern path is 32 percent in the 1-10 MeV neutron flux and 33 percent in the air ionization rate reflecting the nearly factor of ten variation in geomagnetic cutoff during the flight.

Flight 97-107: This was approximately a six & one-half hour flight starting on June 11 at 15:53 on a prescribed southerly heading over the North Pacific ocean (fig. 3). The trajectory was chosen to be approximately normal to the lines of constant geomagnetic cutoffs to maximize the dynamic range of the radiation variation. At the position Latitude 17 deg N, longitude 127 deg 28 min W, the pilot executed a 180 degree turn and returned to base (fig. 20 to 22). The aim of the mission was to obtain radiation measurements as a function of geomagnetic latitude to as far south as reasonably possible and geomagnetic cutoffs of 4.5 to 12.2 GV were obtained (fig. 23). Once altitude was achieved, the environmental quantities declined to nadir at the southern most latitudes as seen in figures 24 to 27. An altitude survey was not attempted since model predictions estimated only a few percent variation in decent to 52,000 ft.

Flight 97-108: This was approximately a six and one-half hour flight starting June 13 at 15:52 on prescribed northern, western, and southern headings similar to flight 105 (fig. 3). The aim was to approximately repeat the radiation measurements as a function of geomagnetic latitude to as far north as possible with altitude excursions along a constant-radiation, geomagnetic latitude line near Edmonton, Canada. The flight (fig. 28 to 30) started at (37 ^{o} 24' N, 122 ^{o} 6' W) with a climb out of Moffett Field. And ascended to cruise altitude and cruised to (54 ^{o} 48' N, 116 ^{o} 48' W). This was followed by a turn west toward (56 ^{o} 00' N, 125 ^{o} W) holding altitude fixed for 5 minutes after the west turn, then executed a medium-rate descent (750 ft/min) to 52,000 ft and maintained at 52,000 ft for 10 minutes (fig.30). At (56 ^{o} 00' N, 125 ^{o} W) the aircraft turned south and ascended to cruise altitude and cruise toward Moffett Field where the flight was ended. The model geomagnetic cutoff, dose equivalent, dose, 1-10 MeV neutron

fluence rates are shown in figures 31 to 35. The northern most geomagnetic cutoff achieved is 0.86 GV compared with 0.43 GV of flight 97-106. It appears that neither the neutron flux nor the ionization rate has reached a plateau as shown in figures 34 and 35.

Flight 97-109: This was a repeat of the first southerly flight 97-107. The aim of this flight was to check data measurement repeatability. There is little difference in the flight trajectory of flight 97-107 with nearly identical model results (fig. 36 to 43).

Comparison to the ion chamber measurement

Since the majority of measured data are being analyzed by each individual laboratory, it may take months or years to obtain the complete results; however one piece of important information; the air ionization rate is readily available. Although the absolute comparison is still not available yet, since the exact dimension, composition of the ion chambers provided by EML and the computer driven data lagging require calibration, the only relation we could establish is the correlation between prediction by AIR model and the measurement and the derivation of an empirical conversion factor from ion chamber output to air ionization rate. The following procedure is adopted. Suppose the predicted set of data is denoted as a_i , the measured bias a function of time measured in minute. Taking ratio

$$c_i = a_i / b_i \tag{10}$$

where a_i is the model air ionization rate and b_i is the ion chamber output we define the average conversion factor as

$$\langle c \rangle = \Sigma\, c_i / N \tag{11}$$

where N is the total number of data points. The resulting estimate of the air ionization rate d_i is then given as

$$d_i = \langle c \rangle\, b_i \tag{12}$$

The actual conversion factor depends on the specific components resulting in ionization and must await a detailed evaluation. Still the present analysis represents a useful preliminary analysis of the flight data. The comparisons of model values a_i with the converted flight data d_i using equation (12) are shown in figures 44 to 48.

Results from flight 97-105 are shown in figure 44. It is seen that the model ionization rates overestimate the air ionization rate by about 3 or 4 percent at these altitudes and geomagnetic cutoffs (R of about 4 GV). A similar overestimate is seen in the first hour of flight 97-106 where the model shows improved agreement for the remainder of the northern leg of the flight. There is a progressive overestimate in the altitude survey at the northern most latitude as seen in figure 45. The return trip shows an underestimate

on the southern leg of less than 5 percent and may reflect irregularities in the geomagnetic field or a temporal fluctuation in the radiation levels. The ion chamber data was stopped abruptly at 400 minutes in the flight. The southern flight (fig. 46) shows the same overestimate near the 4 GV cutoff which extends to lower latitudes followed by an underestimate at the southern terminus of the flight. Again differences are on the order of 5 percent. The second northern flight 97-108 shows the same overestimate near 4 GV with reasonable agreement elsewhere even on the return leg (fig. 47). This would indicate that the underestimate on the southern leg of flight 97-106 is probably not a problem with the geomagnetic cutoff but may be an intensity fluctuation in solar modulation. These issues need to be further studied. The results of flight 97-109 in fig. 49 are almost an exact repeat of flight 97-107. It is clear that the air ionization within the AIR model version 0 is probably accurate to better than 5 percent and could be improved. There is evidence of a temporal fluctuation on the order of a few percent that will be pursued in a latter analysis.

Concluding Remark

The AIR ER-2 flight measurements is a one of the first attempts to a relatively complete measurement of the high altitude radiation level environment. The primary thrust is to characterize the atmospheric radiation components and to later define risk levels at high altitude flight. A secondary thrust is to develop and validate dosimetric techniques and monitoring devices for protecting aircrews. The present analysis of the AIR ion chamber represents about 40 percent of the health risk. We are quite pleased that preliminary results are rather encouraging that the measured physical quantities and our model predicted values do agree well. As more measured values are revealed, we will gain more understanding about our harzadous radiation environment and acquire more confidence in our prediction models.

References

FAA Advisory Committee on the Radiobiological Aspects of the Supersonic Transport, Cosmic radiation exposure in the Supersonic and subsonic flight. Aviat., Space & Environ. Med. 46:1170-1185; 1975

Foelsche, T., Mendell, R.B., Wilson, J.W., Adams, R.R., Measured and calculated neutron spectra and dose equivalent rates at high altitudes: Relevance to SST operations and space research. NASA TN D-7715, 1974

NCRP, Limitation of exposure to ionizing radiation. NCRP Rep. No. 116, 1993.

NCRP, Radiation Exposure and High-Altitude Flight. NCRP Commentary No. 12, July 21, 1995.

O'Brien ,K., Friedberg, W., Atmospheric cosmic rays at aircraft altitudes. Environ. Intern. 20:645-663; 1994.

Schaefer, H.J., Public health aspects of galactic radiation exposures at supersonic transport altitudes. Aerosp. Med. 39:1298-1303; 1968.

Wilson, J. W., et al., Transport Methods and Interactions for Space Radiation, NASA RP-1257, 1991.

Table 1. Ionization Rates in Air Measured by Argon-Filled Chambers[1]
at Solar Minimum (C = 98.3 in 1965)

Ion pairs, cm-3_sec-1, for air depths, g/cm2, of

R, GV	30	40	50	60	70	80	90	100	120	140	200	245	300	1034
0	445.0	430.0	414.0	399.0	383.0	366.0	349.0	332.0	298.0	266.0	181.0	136.0	95.0	11.4
.01	445.0	430.0	414.0	399.0	383.0	366.0	349.0	332.0	298.0	266.0	181.0	136.0	95.0	11.4
.16	444.0	430.0	414.0	399.0	383.0	366.0	349.0	332.0	298.0	266.0	181.0	136.0	95.0	11.4
.49	411.8	404.3	394.4	382.0	369.0	354.8	339.4	325.0	292.3	264.5	181.0	136.0	95.0	11.4
1.31	390.0	385.0	380.0	370.0	365.0	350.0	335.0	320.0	290.0	264.0	181.0	135.0	95.0	11.4
1.97	325.0	333.0	340.0	335.0	330.0	312.5	308.0	300.0	285.0	264.0	181.0	134.0	95.0	11.4
2.56	300.0	305.0	310.0	305.0	300.0	290.0	285.0	280.0	255.0	230.0	173.0	126.0	95.0	11.4
5.17	185.0	195.0	208.0	208.0	208.0	208.0	208.0	208.0	195.0	185.0	135.0	103.0	75.0	10.6
8.44	127.6	137.0	145.0	150.2	153.8	155.8	156.0	154.6	149.7	142.2	111.3	87.0	66.6	10.4
11.70	85.0	92.0	98.0	100.0	102.0	105.0	107.0	110.0	108.0	105.0	80.0	77.0	60.0	10.0
14.11	70.0	75.0	82.0	85.0	89.0	93.6	95.0	100.0	98.0	95.0	78.0	68.8	50.0	10.0
17.00	66.3	73.8	80.0	84.8	88.5	91.1	92.6	93.5	93.4	90.5	75.0	62.3	48.0	10.0

[1]Experimental data extrapolated to provide estimates of ionization rates over a wide range of altitudes and geomagnetic cutoffs.

Table 2. Ionization Rates in Air Measured by Argon-Filled Chambers[1]
at Solar Maximum (C = 80 in 1958)

Ion pairs, cm-3_sec-1, for air depths, g/cm2, of

R, GV	30	40	50	60	70	80	90	100	120	40	00	45	300	1034
0	264.6	267.5	267.0	265.0	258.0	252.0	243.0	235.0	216.3	197.0	145.0	109.2	78.8	11.4
.01	264.6	267.8	267.0	265.0	258.0	251.0	243.0	235.0	216.3	197.0	145.0	109.2	78.8	11.4
.16	264.0	264.9	265.0	264.0	257.0	250.0	243.0	233.0	215.0	197.0	145.0	109.2	78.8	11.4
.49	264.0	264.9	265.0	262.0	256.0	249.0	242.0	231.0	213.2	197.0	145.0	109.2	78.8	11.4
1.31	264.0	265.0	265.0	262.0	253.0	247.0	241.0	231.0	213.0	197.0	145.0	108.0	78.8	11.4
1.97	264.0	265.0	265.0	262.0	252.0	245.0	241.0	231.0	212.5	197.0	145.0	107.8	78.8	11.4
2.56	235.0	237.5	240.0	240.0	239.0	238.0	237.0	230.0	209.0	197.0	145.0	101.6	78.8	11.4
5.17	162.5	168.0	179.0	182.0	178.0	175.2	174.0	173.8	170.0	160.0	159.0	88.3	65.0	10.6
8.44	95.0	103.5	112.0	118.0	118.0	119.0	120.0	122.0	118.0	117.0	100.6	78.7	60.2	10.4
11.70	78.2	85.0	90.7	92.7	94.8	98.0	100.0	103.1	101.2	98.4	75.0	72.2	56.2	10.0
14.11	65.7	70.7	77.5	80.5	84.3	89.0	90.5	95.3	93.5	90.9	74.0	65.9	47.9	10.0
17.0	63.0	70.3	76.4	81.1	84.8	87.5	89.1	90.2	90.1	87.4	72.6	60.3	46.5	10.0

[1]Experimental data extrapolated to provide estimates of ionization rates over a wide range of altitudes and geomagnetic cutoffs.

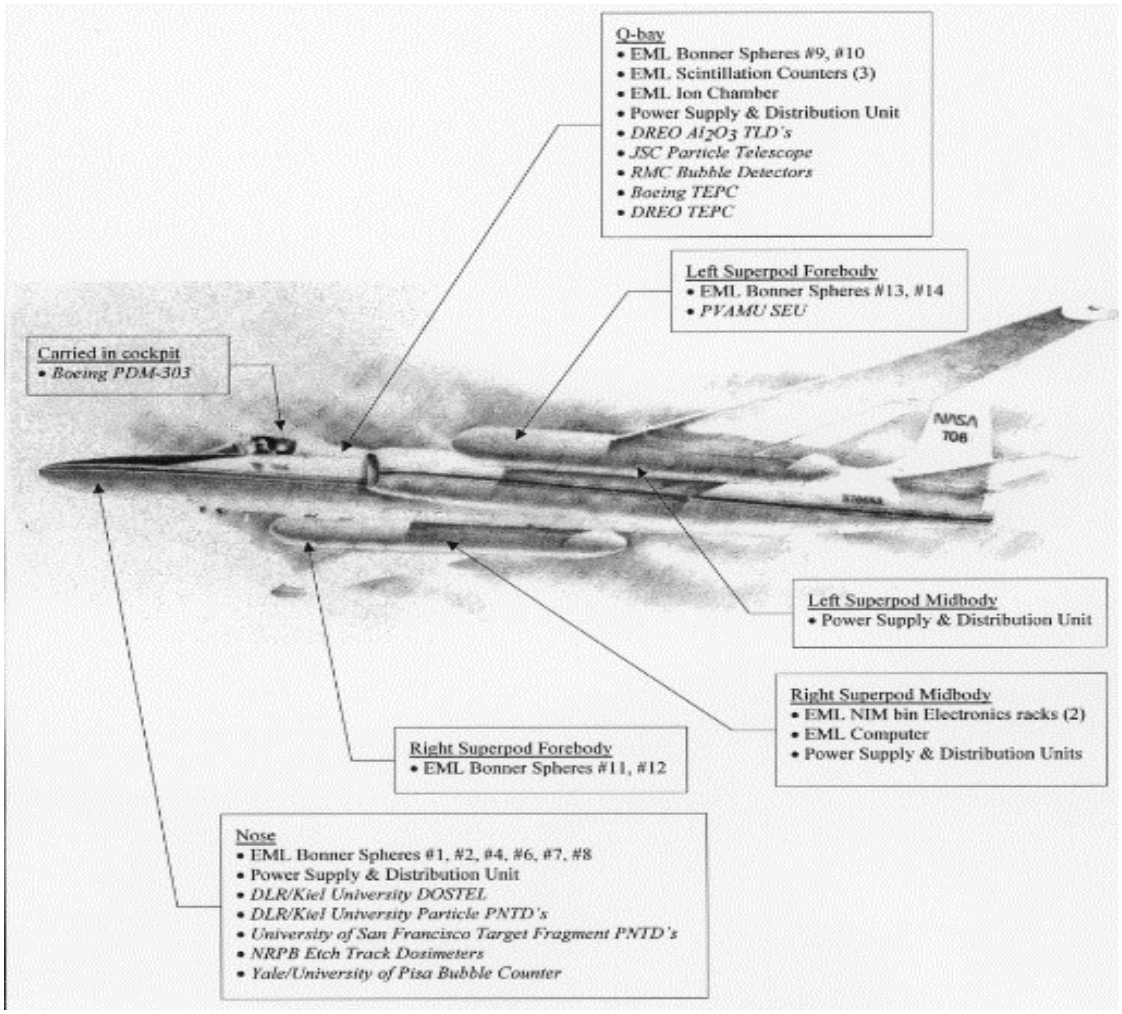

Figure 1.- Instrument Locations on the ER-2.

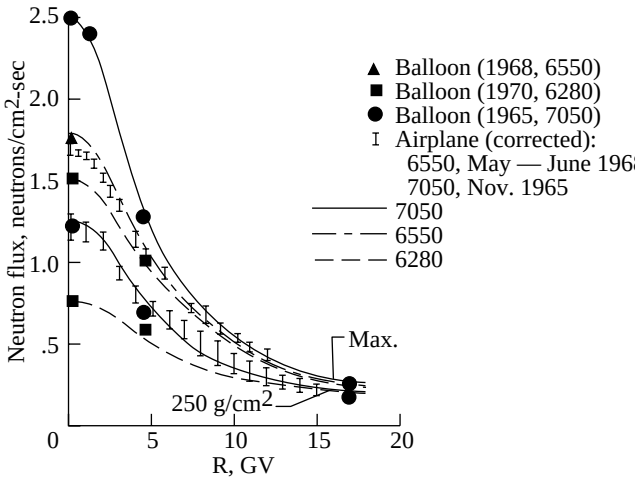

Figure 2. Fast neutron flux (in range from 1 to 10 MeV) at the transition maximum an 240-g/cm^2 depth as a function of vertical cutoff rigidity *R* for various times in the solacycle and DRNM count rates.

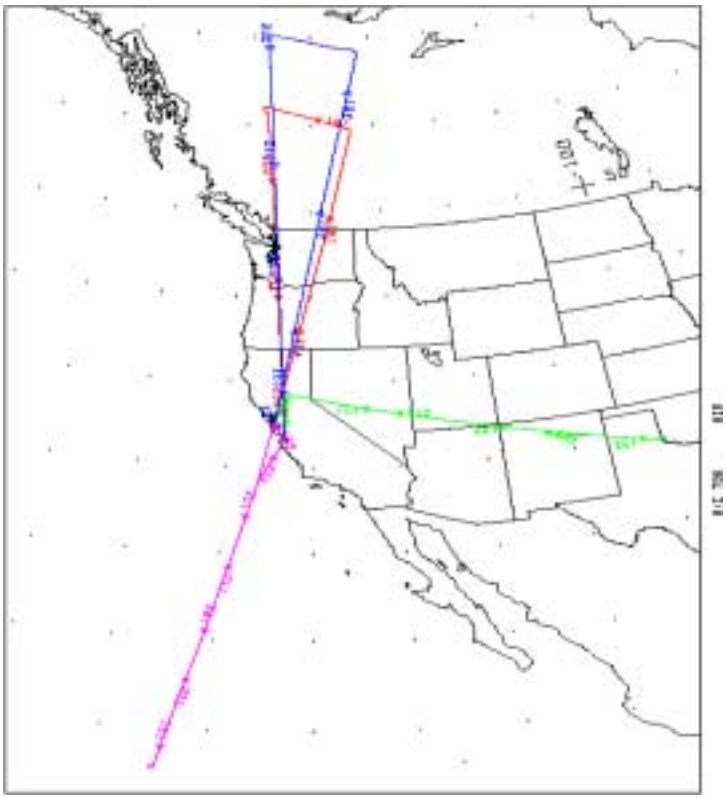

Figure 3. Ground tracks of flights 97-105 to 97-109.

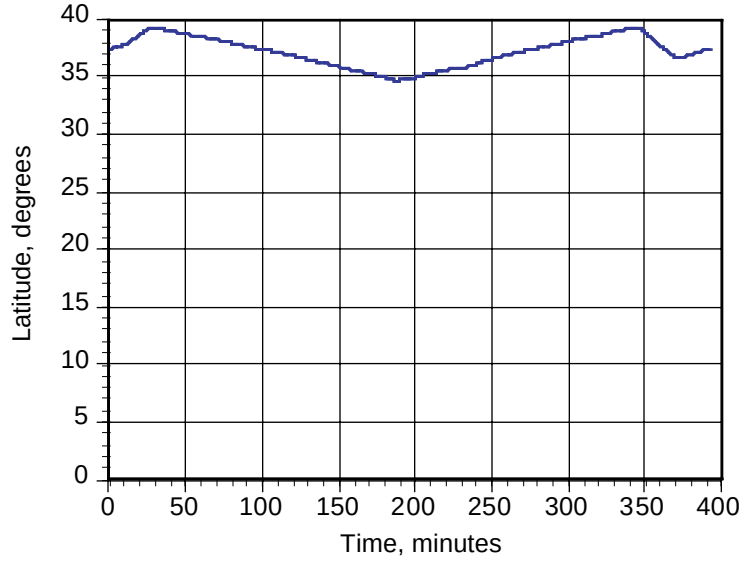

Fig. 4 Latitude of flight path as function of Time for Flight 97-105

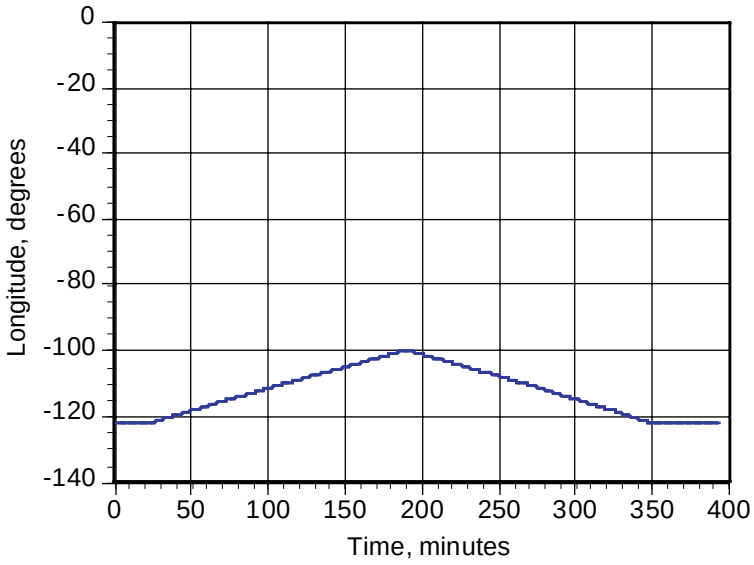

Fig. 5 Longitude of flight path as function of time for Flight 97-105

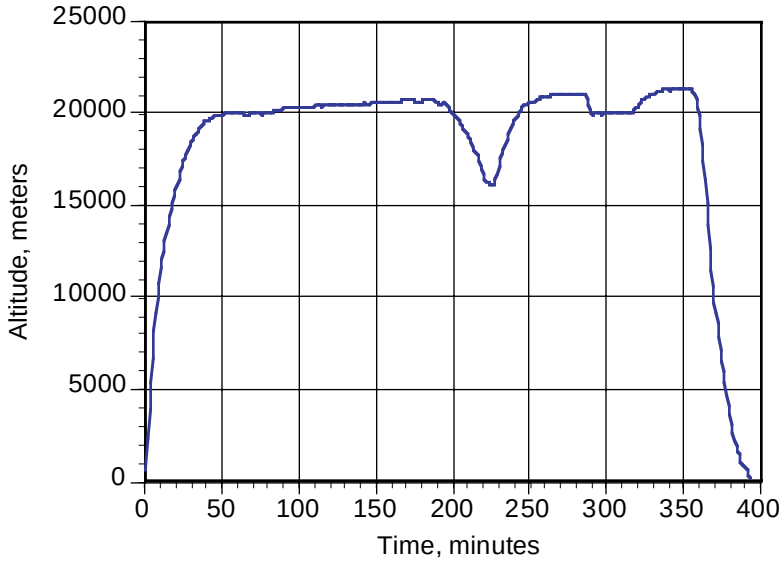

Fig. 6 Altitude of flight path as function of time for Flight 97-105

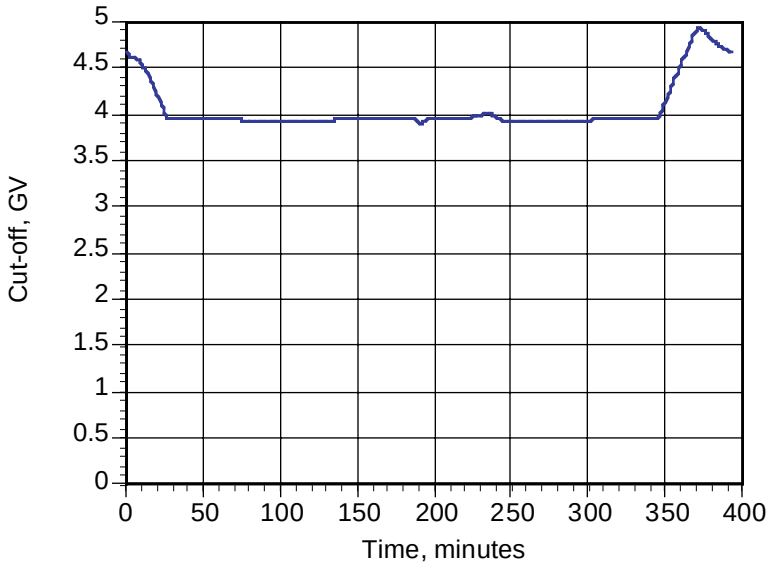

Fig. 7 Magnetic cut-off of flight path as function of time for Flight 97-105

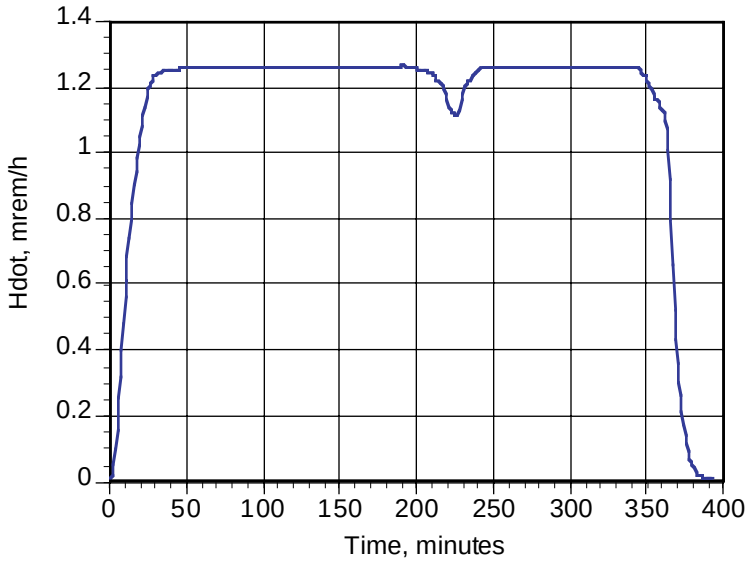

Fig. 8 Dose Equivalent Rate as function of time for Flight 97-105

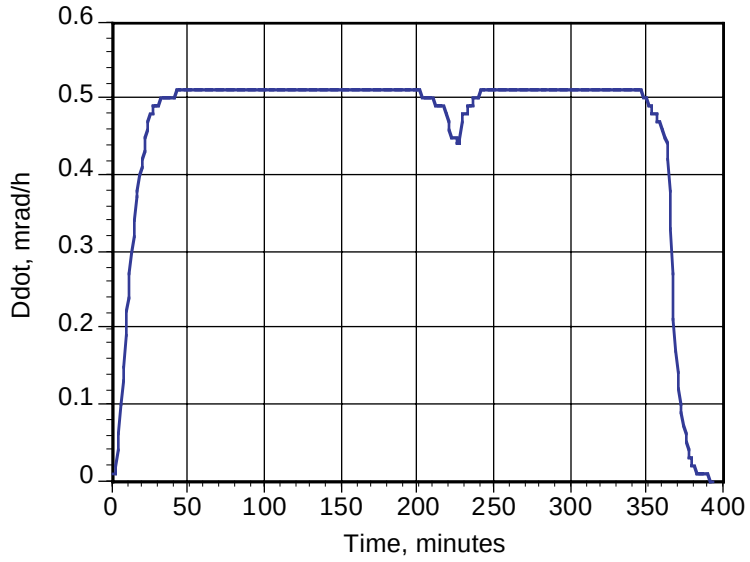

Fig. 9 Dose Rate as function of time for Flight 97-105

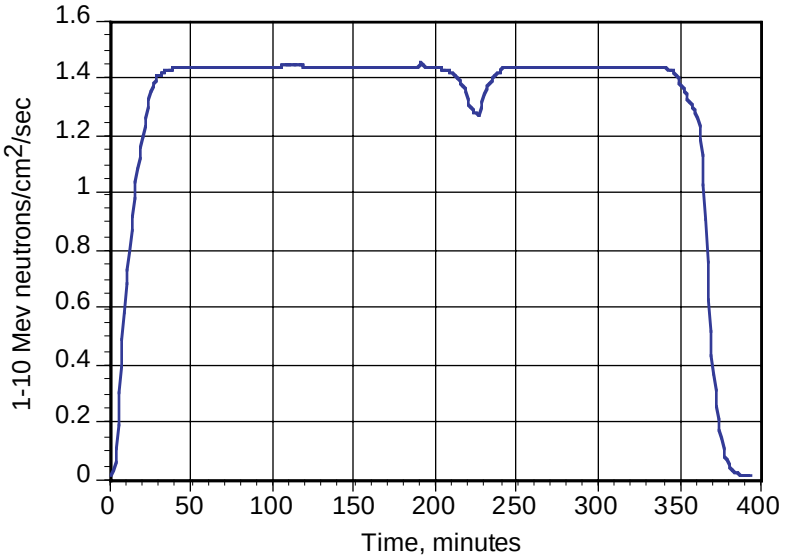

Fig. 10 Neutron Flux as function of time for Flight 97-105

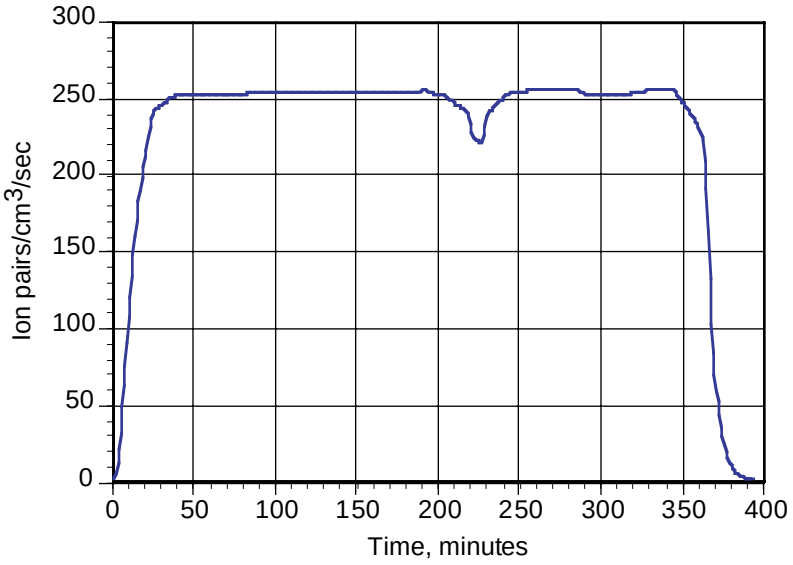

Fig. 11 Air Ionization Rate as function of time for Flight 97-105

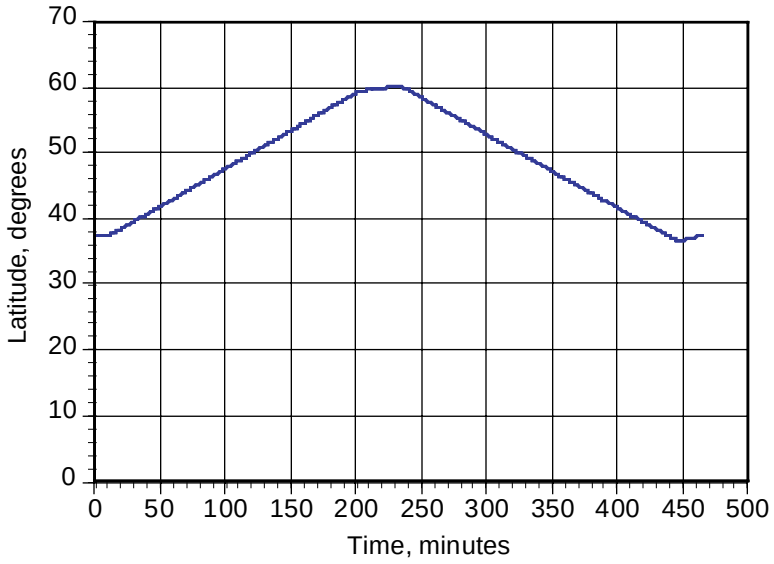

Fig. 12 Latitude of flight path as function of time for Flight 97-106

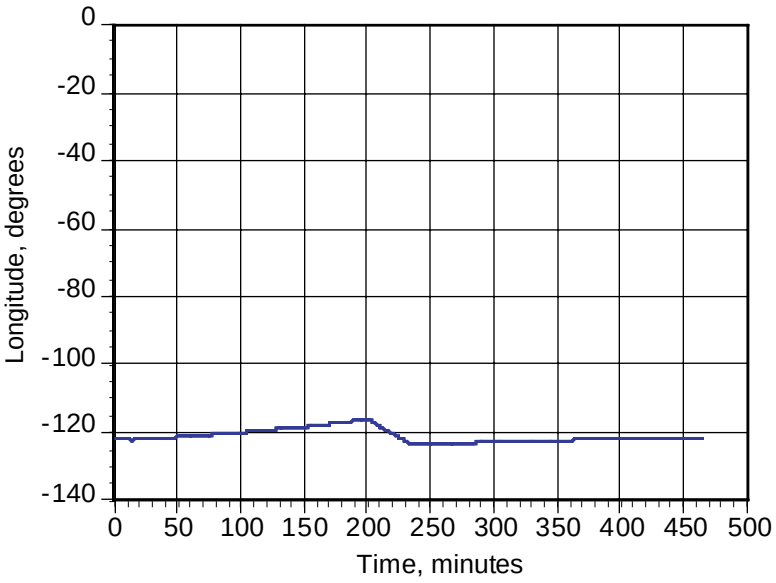

Fig. 13 Longitude of flight path as function of time for Flight 97-106

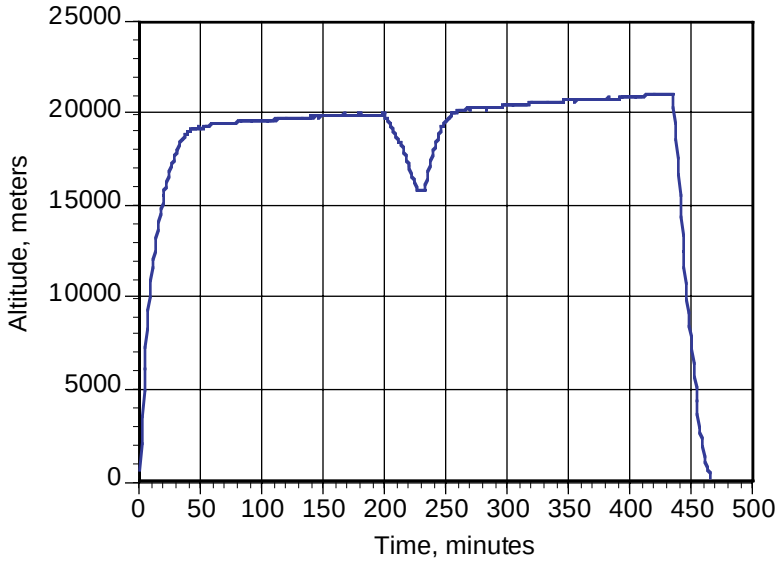

Fig. 14 Altitude of flight path as function of time for Flight 97-106

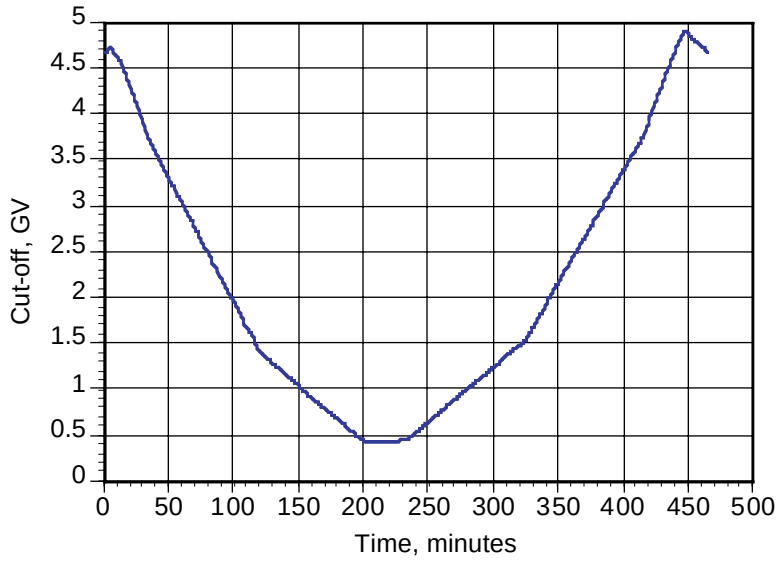

Fig. 15 Magnetic cut-off of flight path as function of time for Flight 97-106

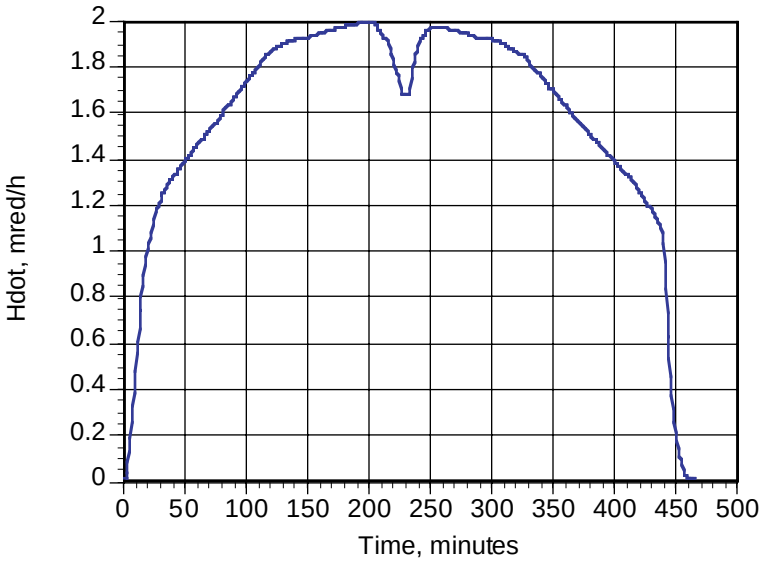

Fig.16 Dose Equivalent Rate as function of time for Flight 97-106

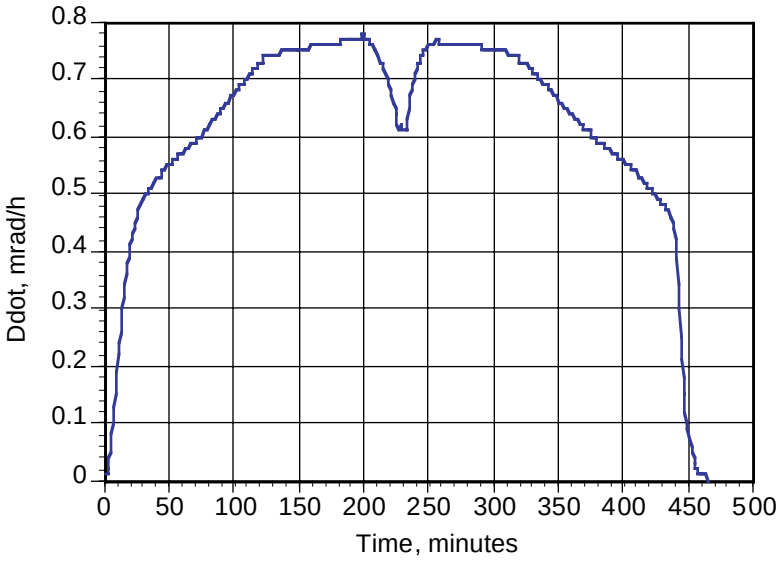

Fig.17 Dose Rate as function of time for Flight 97-106

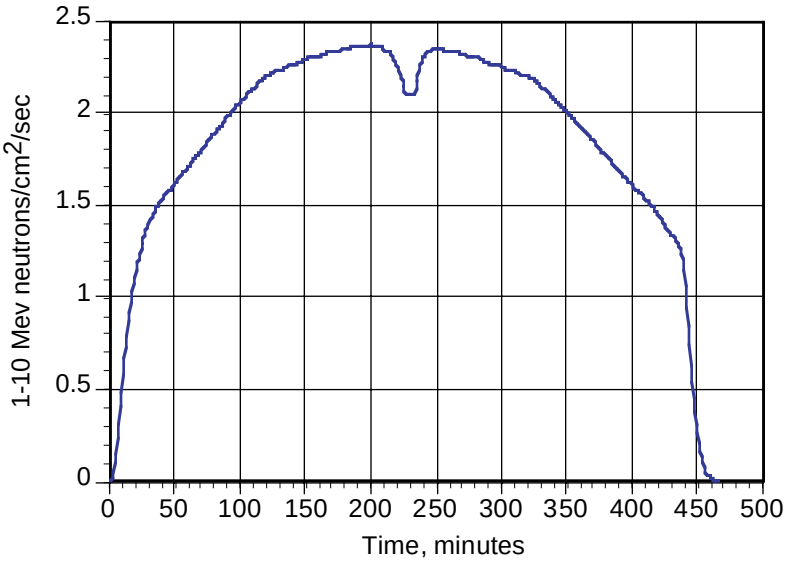

Fig.18 Neutron Flux as function of time for Flight 97-106

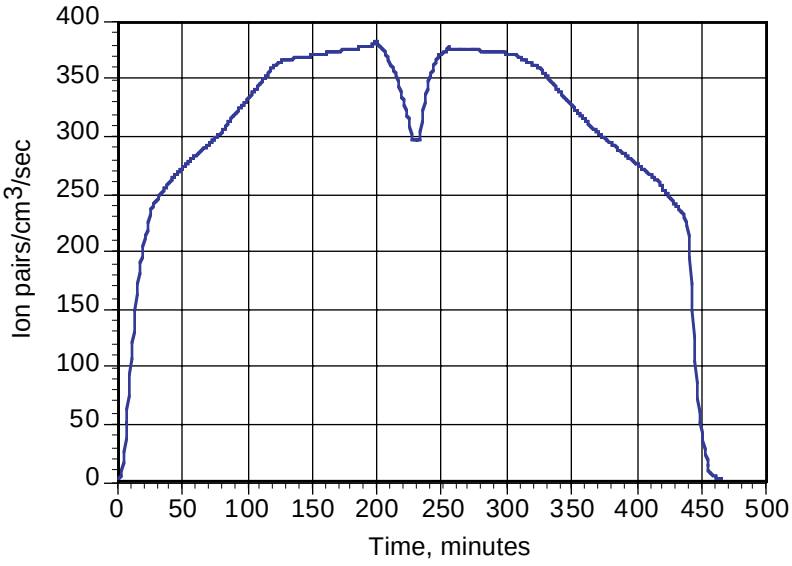

Fig.19 Air Ionization Rate as function of time for Flight 97-106

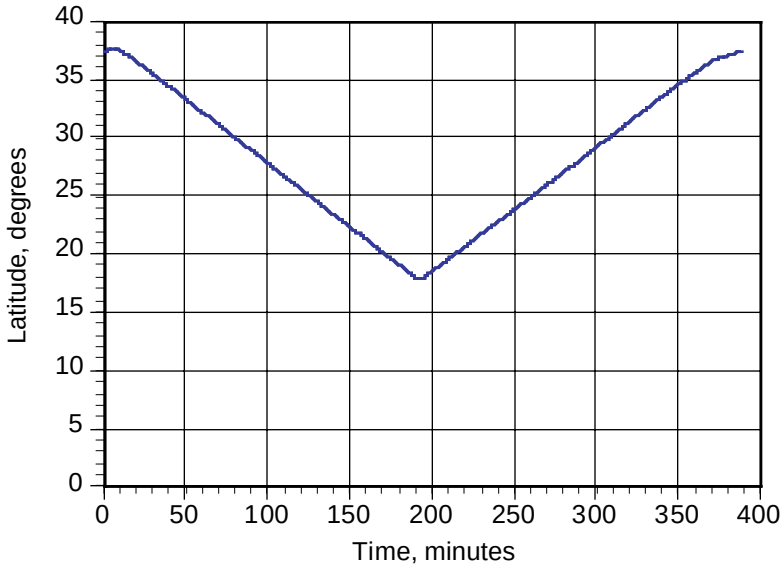

Fig. 20 Latitude of flight path as function of time for Flight 97-107

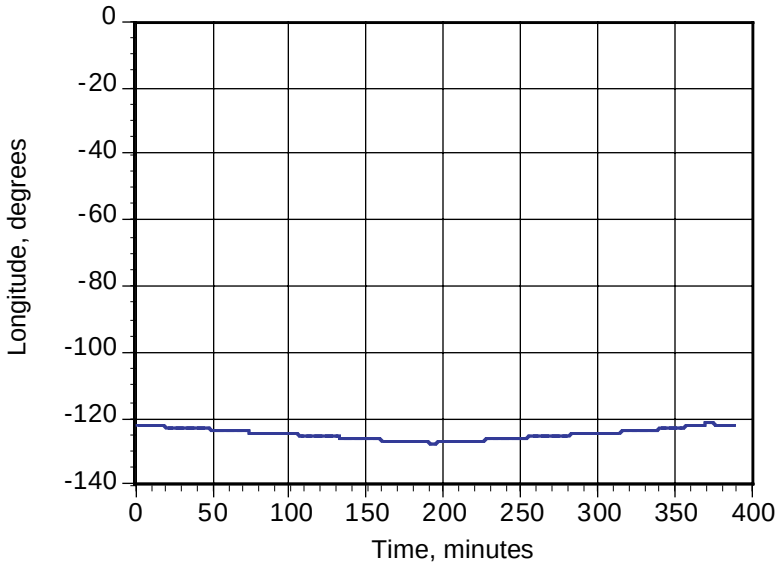

Fig. 21 Longitude of flight path as function of time for Flight 97-107

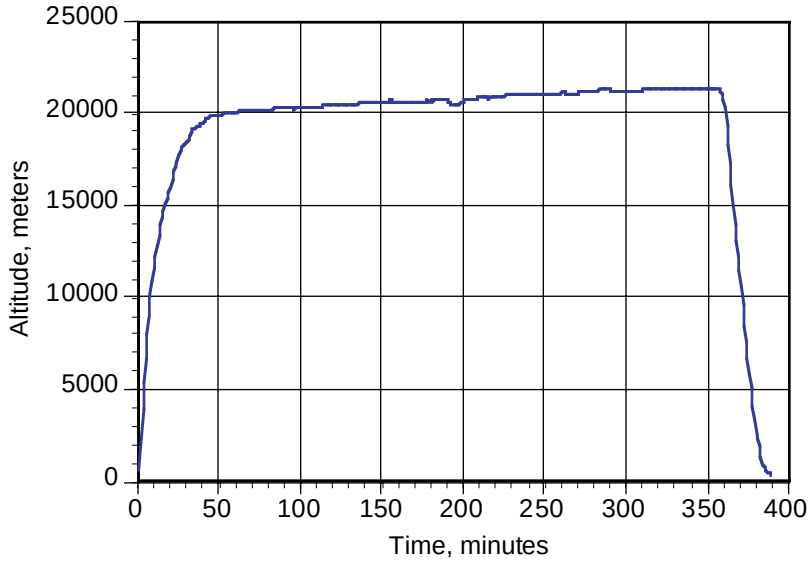

Fig. 22 Altitude of flight path as function of time for Flight 97-107

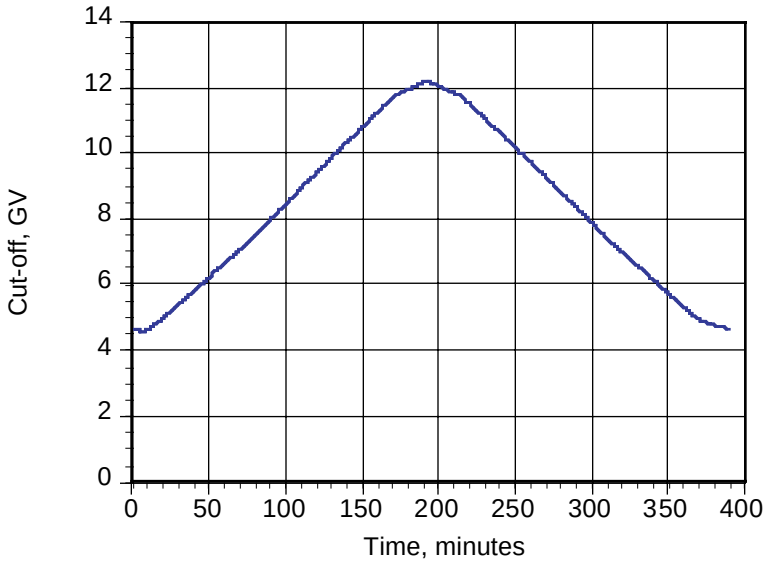

Fig. 23 Magnetic cut-off of flight path as function of time for Flight 97-107

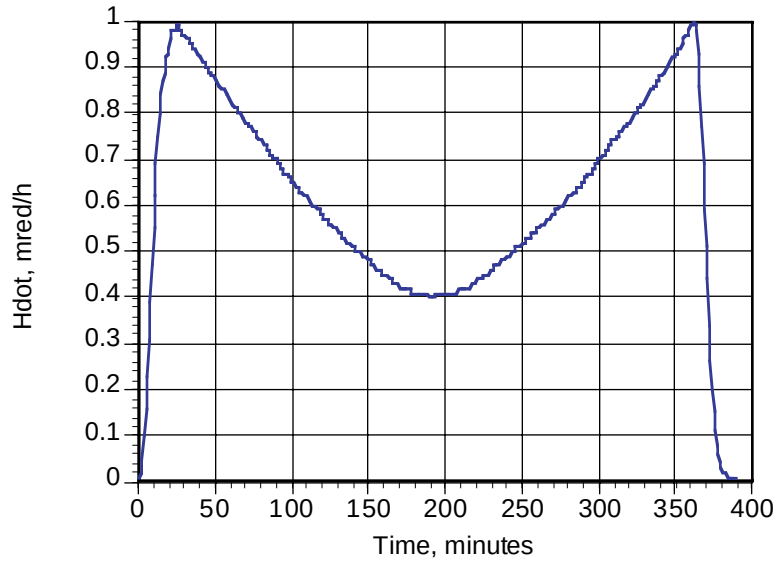

Fig.24 Dose Equivalent Rate as function of time for Flight 97-107

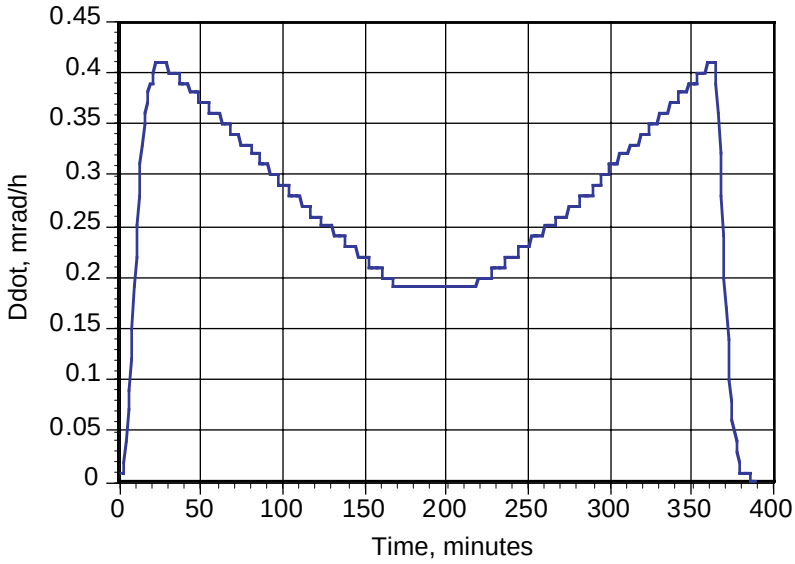

Fig.25 Dose Rate as function of time for Flight 97-107

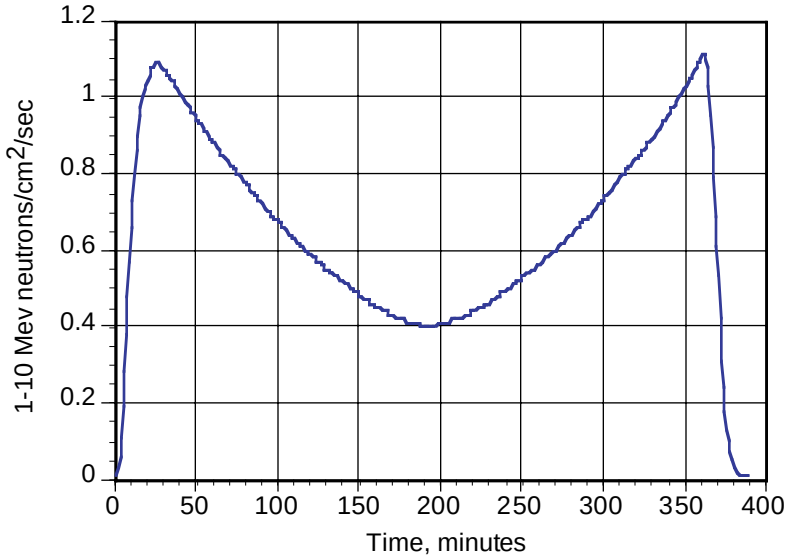

Fig. 26 Neutron Flux as function of time for Flight 97-107

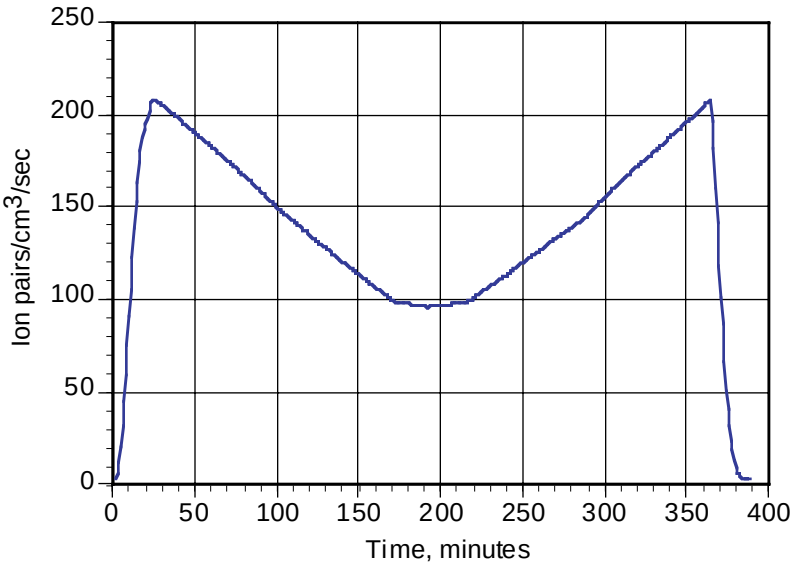

Fig.27 Air Ionization Rate as function of time for Flight 97-107

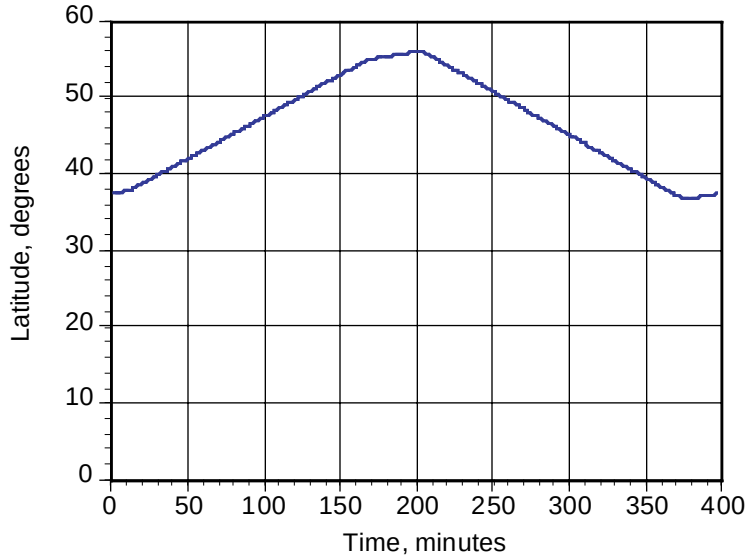

Fig. 28 Latitude of flight path as function of time for Flight 97-108

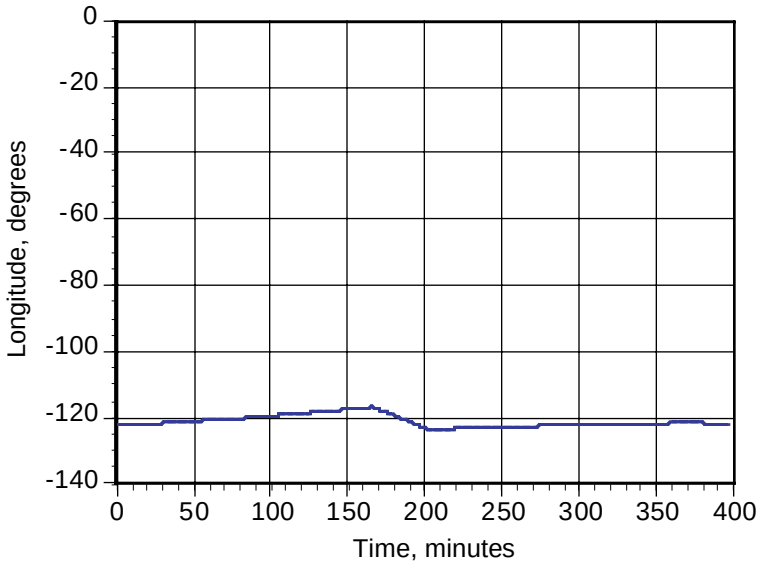

Fig. 29 Longitude of flight path as function of time for Flight 97-108

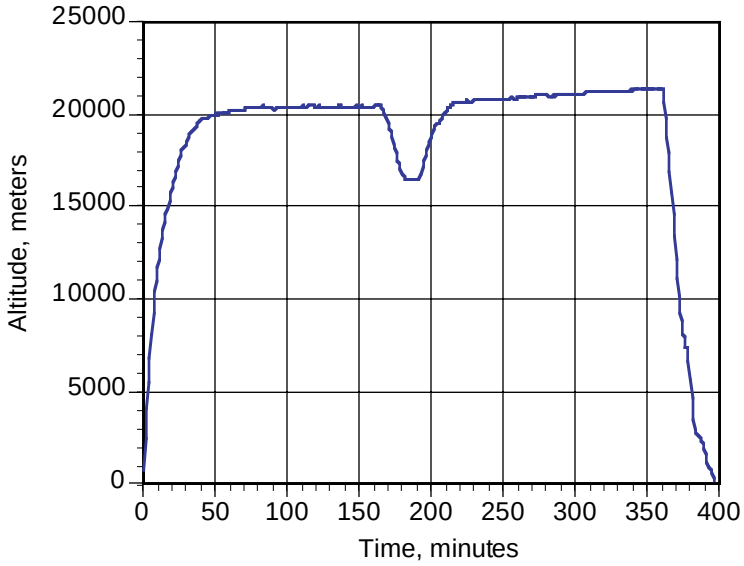

Fig. 30 Altitude of flight path as function of time for Flight 97-108

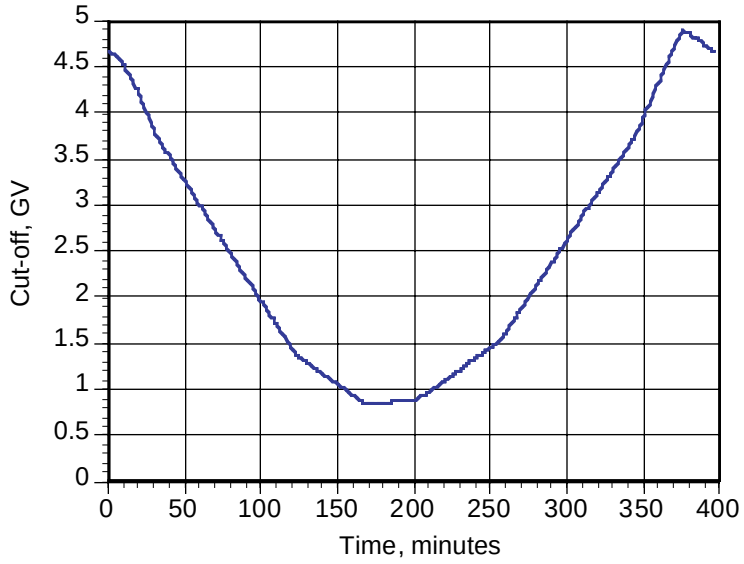

Fig. 31 Magnetic cut-off of flight path as function of time for Flight 97-108

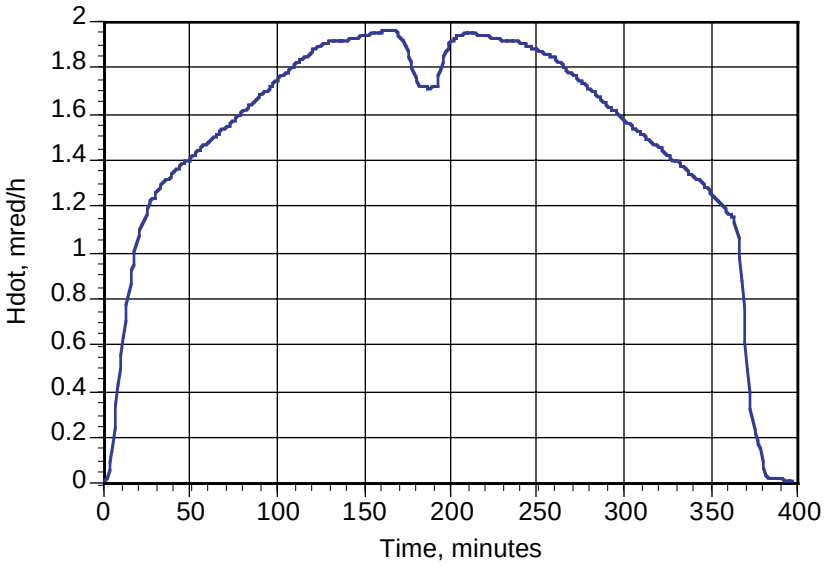

Fig.32 Dose Equivalent Rate as function of time for Flight 97-108

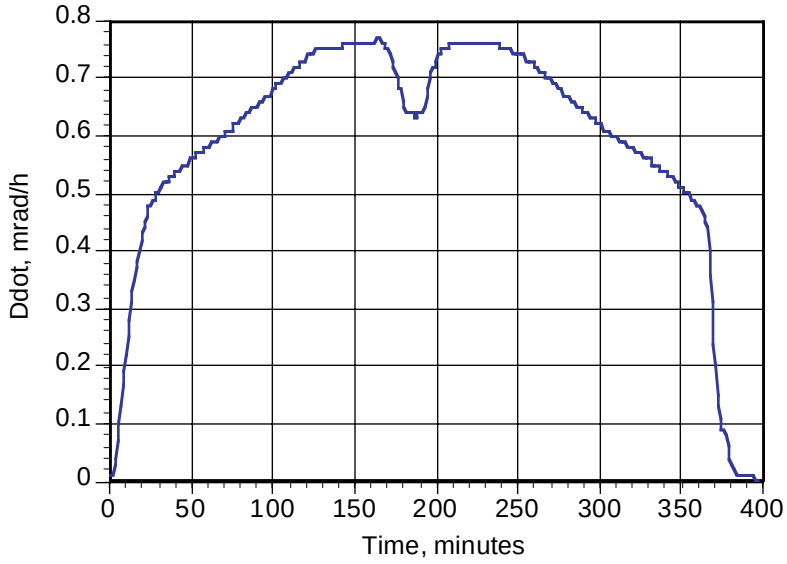

Fig.33 Dose Rate as function of time for Flight 97-108

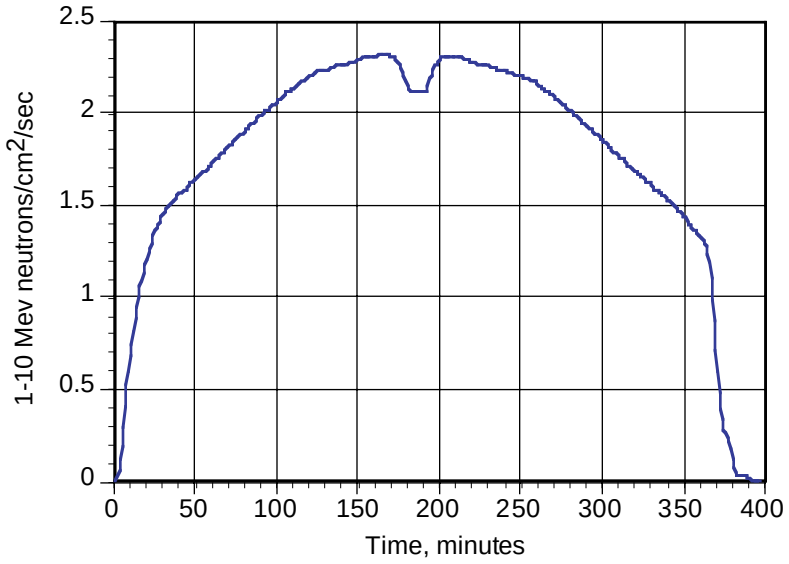

Fig.34 Neutron Flux as function of time for Flight 97-108

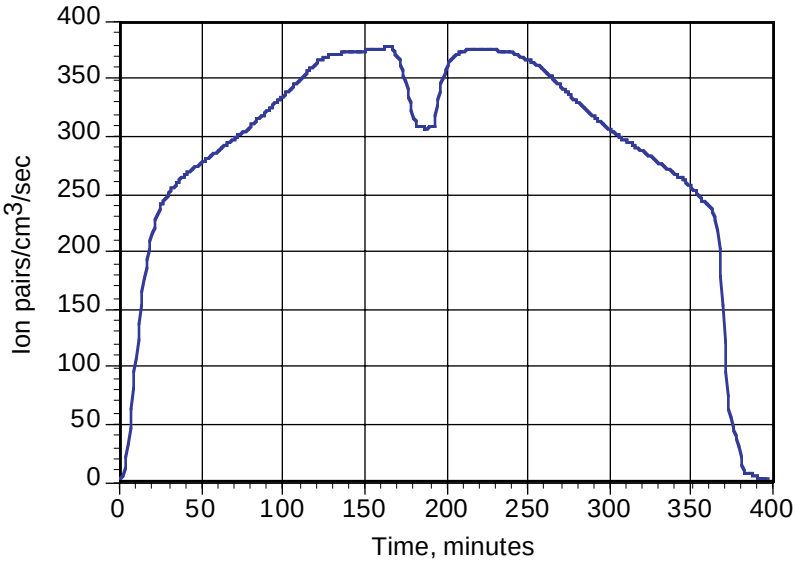

Fig. 35 Air Ionization Rate as function of time for Flight 97-108

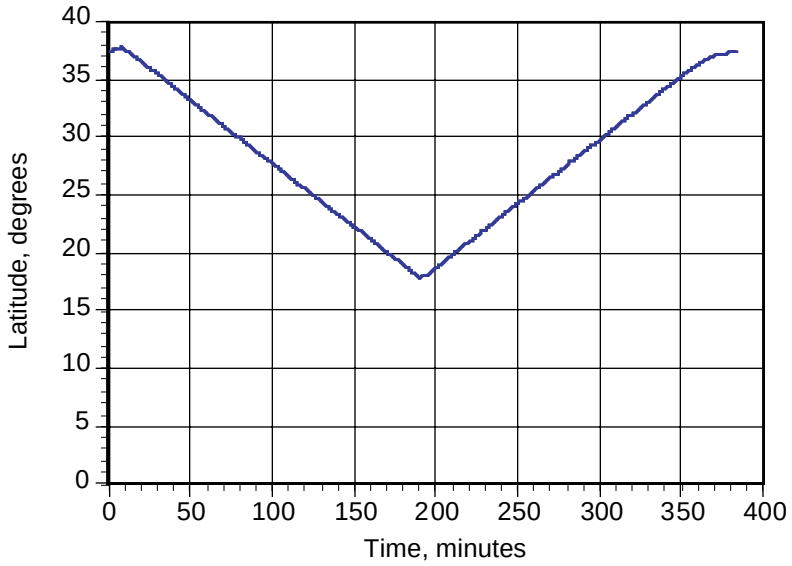

Fig. 36 Latitude of flight path as function of time for Flight 97-109

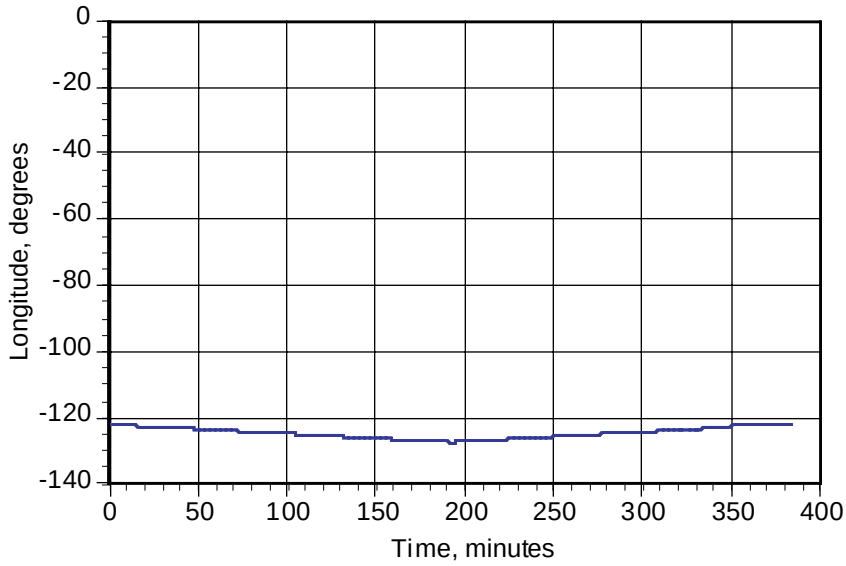

Fig. 37 Longitude of flight path as function of time for Flight 97-109

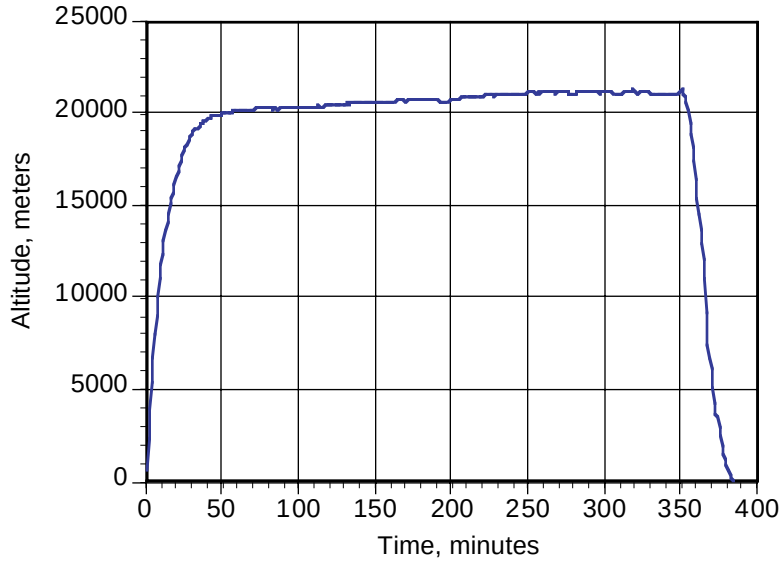

Fig. 38 Altitude of flight path as function of time for Flight 97-109

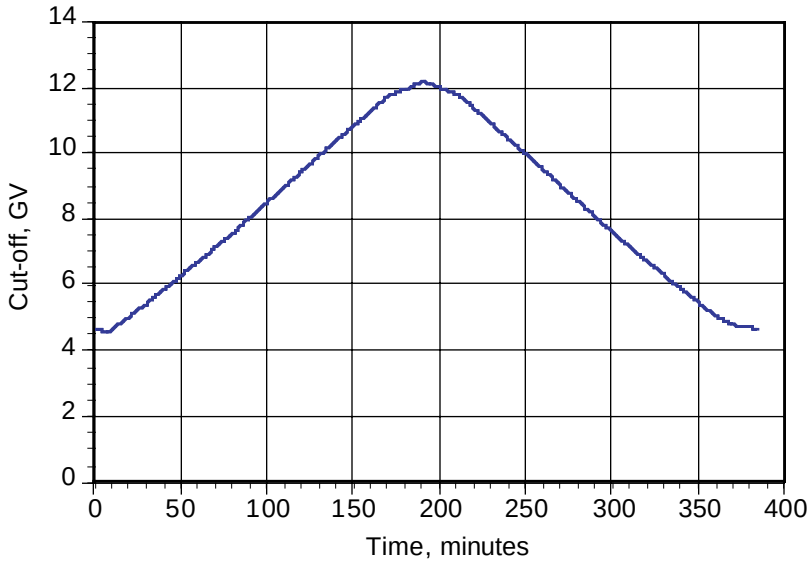

Fig. 39 Magnetic cut-off of flight path as function of time for Flight 97-109

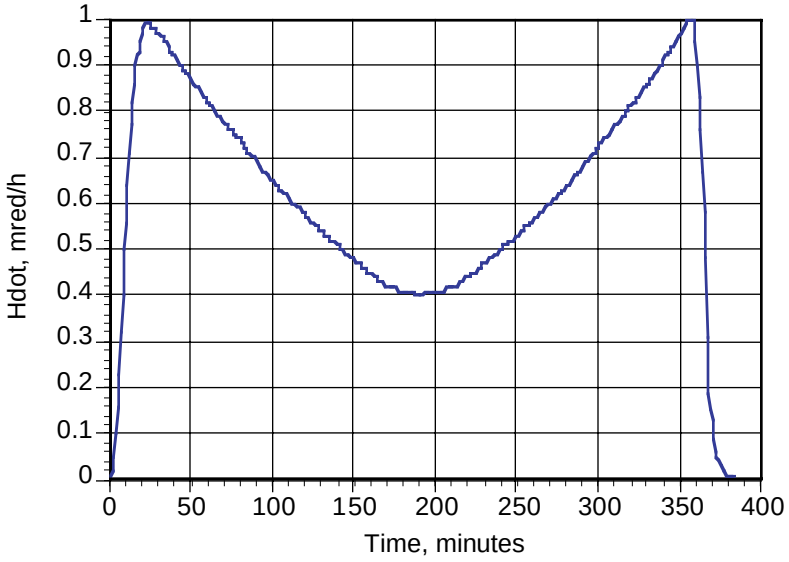

Fig.40 Dose Equivalent Rate as function of time for Flight 97-109

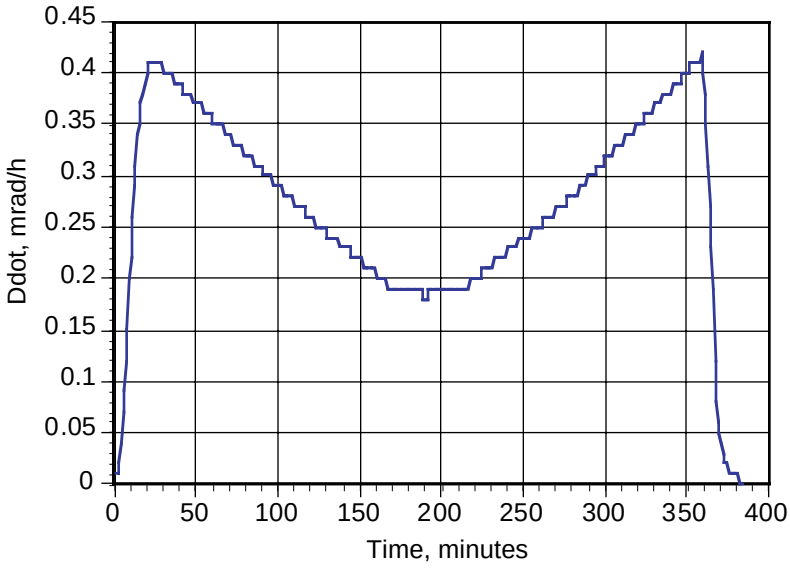

Fig.41 Dose Rate as function of time for Flight 97-109

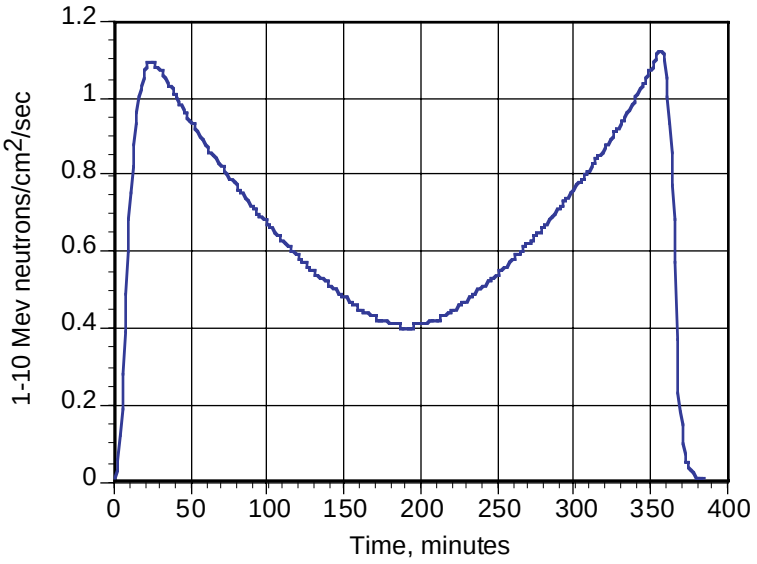

Fig.42 Neutron Flux as function of time for Flight 97-109

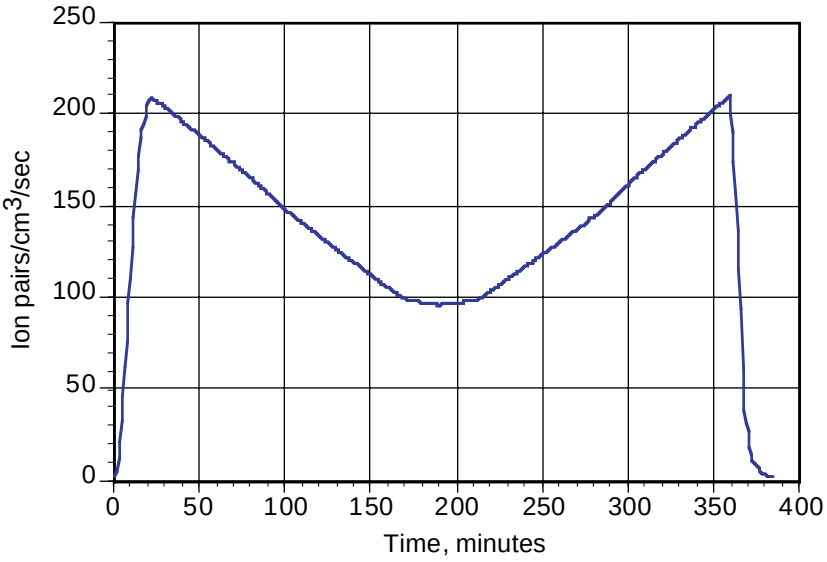

Fig.43 Air Ionization Rate as function of time for Flight 97-109

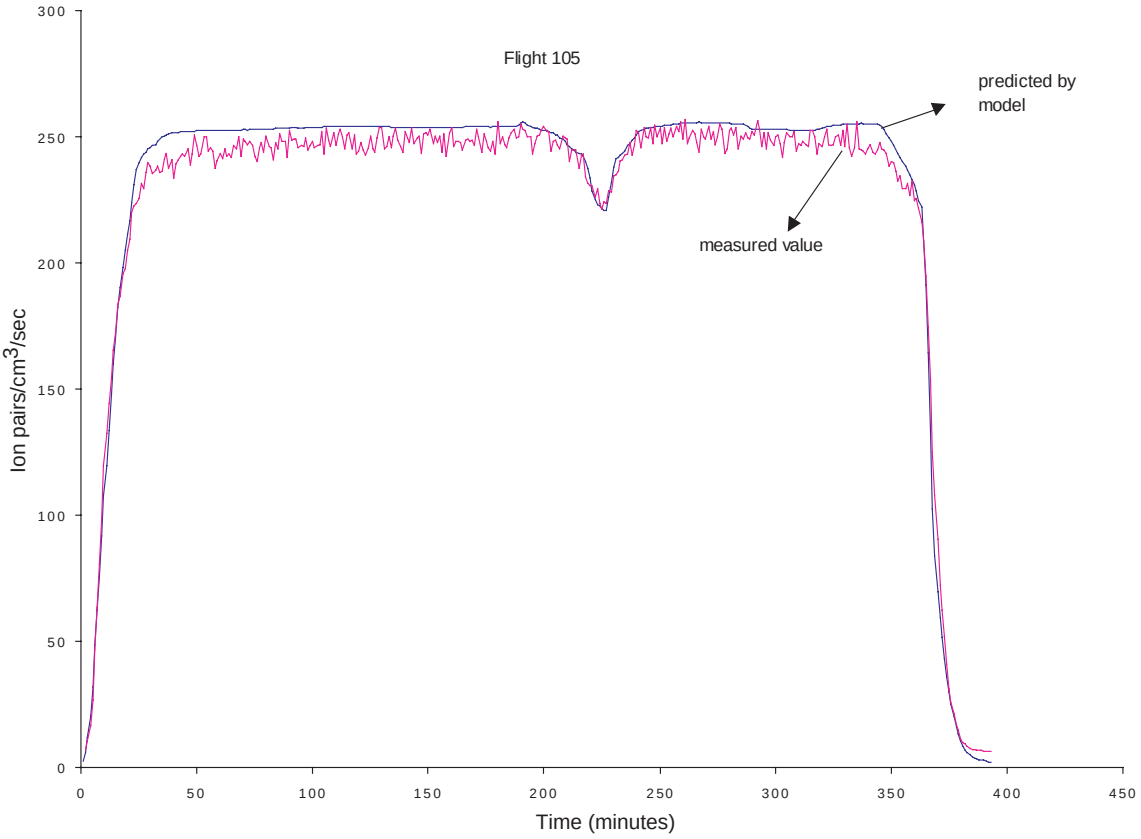

Fig. 44 Predicted and measured value of Air Ionization Rate as function of time for Flight 97-105

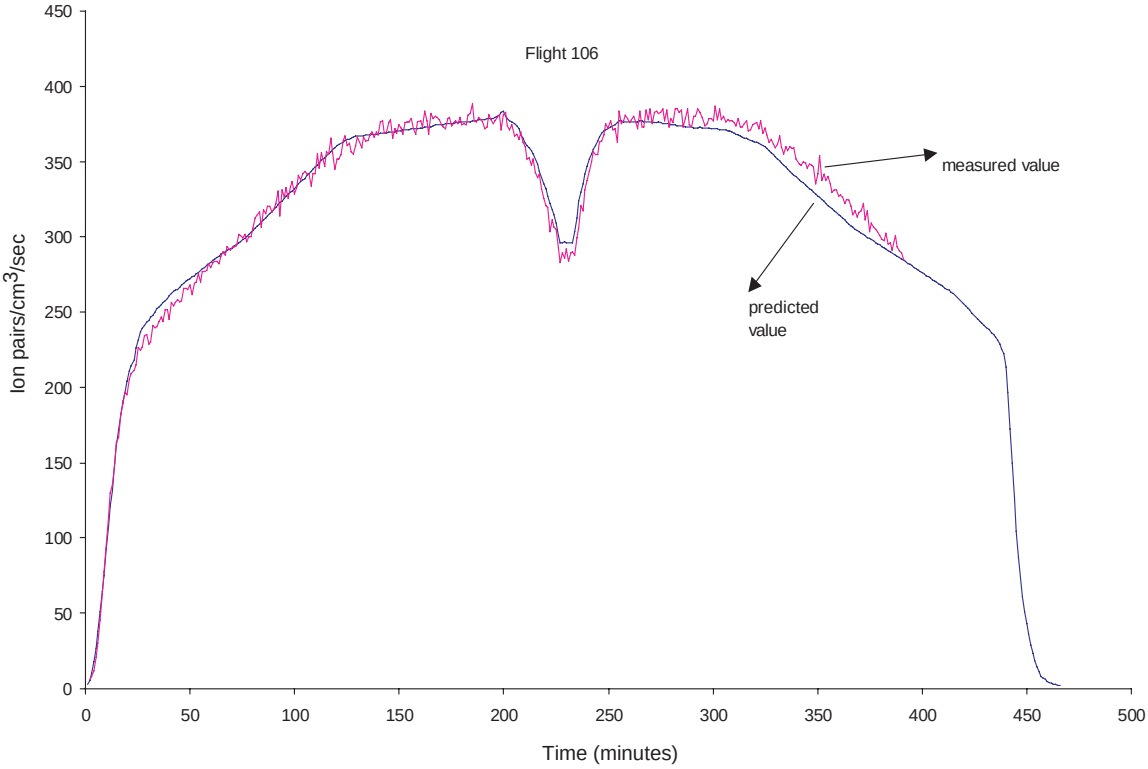

Fig. 45 Predicted and measured value of Air Ionization Rate as function of time for Flight 97-106

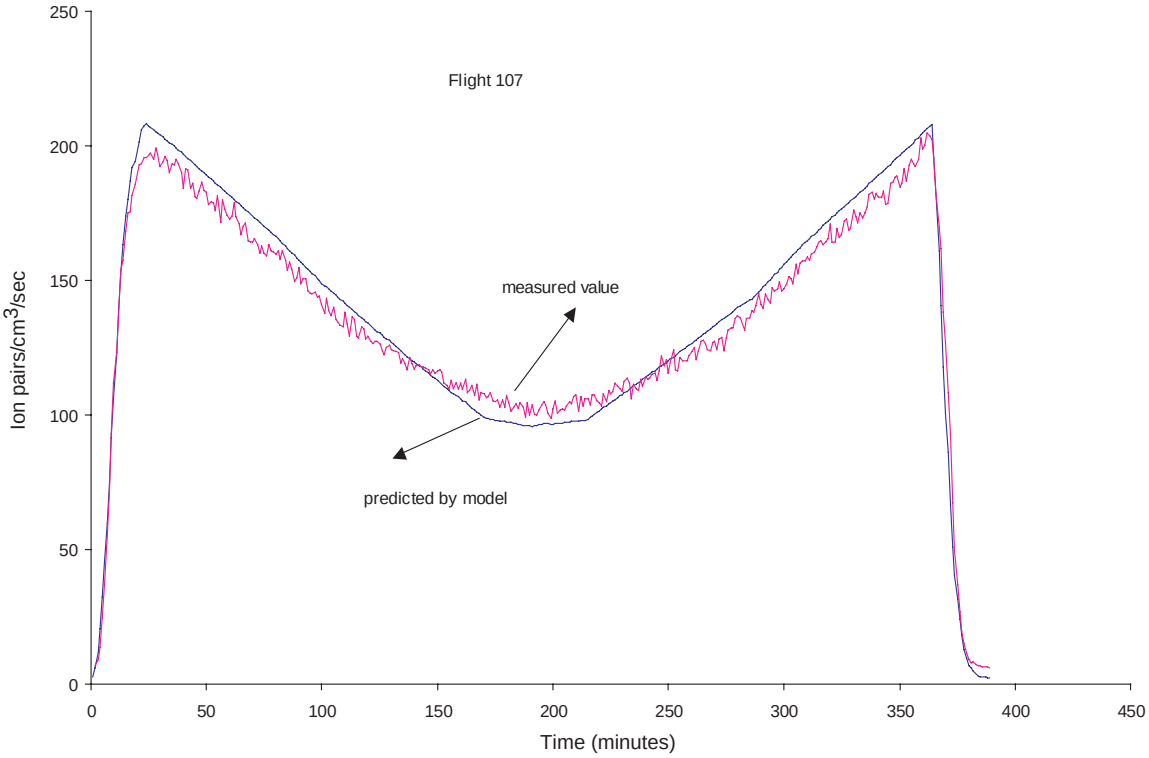

Fig. 46 Predicted and measured value of Air Ionization Rate as function of time for Flight 97-107

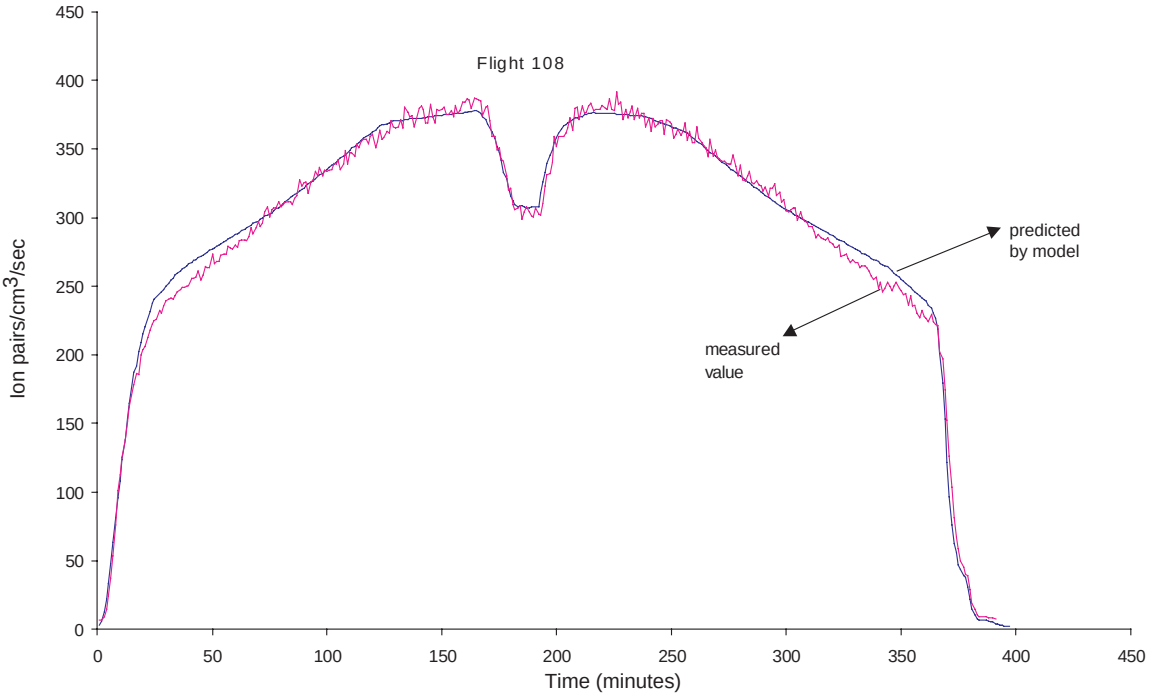

Fig 47 Predicted and measured value of Air Ionization Rate as function of time for Flight 97-108

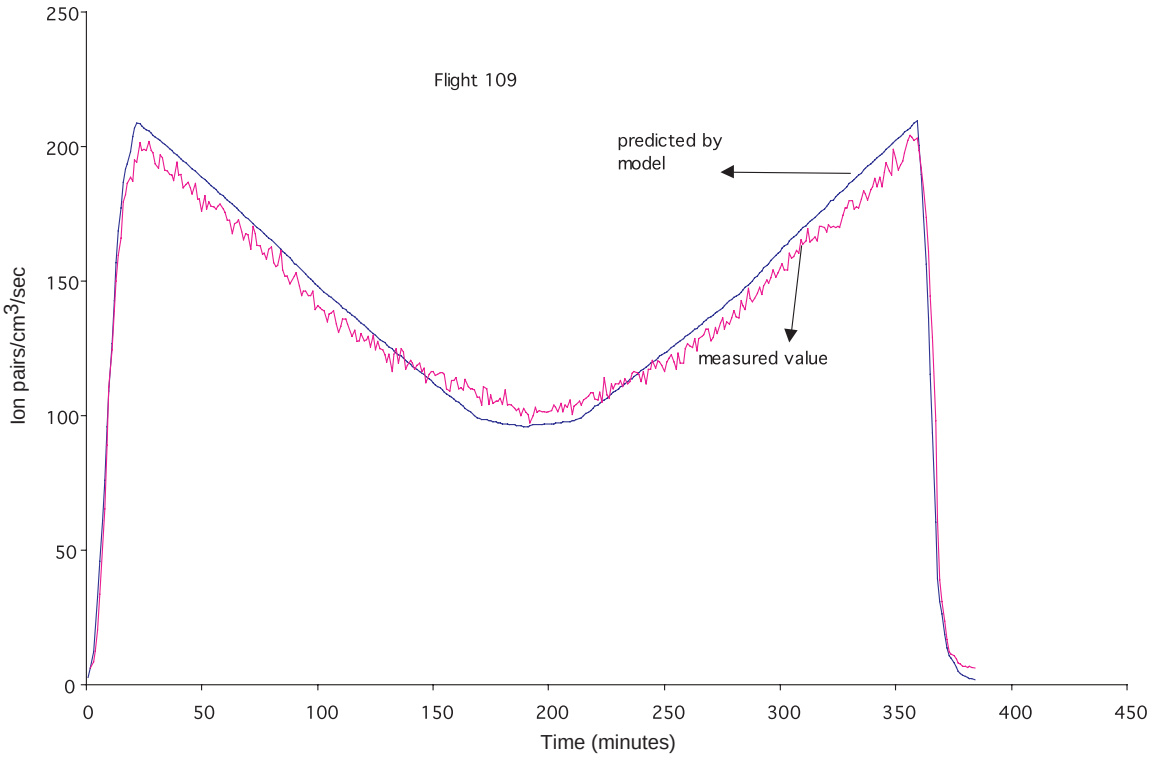

Fig. 48 Predicted and measured value of Air Ionization Rate as function of time for Flight 97-109.